NEUROSCIENCE RESEARCH NOTES

OPEN ACCESS | TECHNICAL NOTES ISSN: 2576-828X

Construction and validation of over-expression of RE1-silencing transcription factor (REST) using PiggyBac transposon inducible vector system in HEK293FT cells

Norhazlin Jusoh [1,2], Norshariza Nordin [1,3], Nurul Ain Nasim Mohd Yusof [4], Pike-See Cheah [3,5] and King-Hwa Ling [1,3]*

[1] Department of Biomedical Sciences, Faculty of Medicine and Health Sciences, Universiti Putra Malaysia, 43400 Serdang, Selangor, Malaysia.
[2] Faculty of Applied Sciences, Universiti Teknologi MARA, Perak Branch, Tapah Campus, 35400 Tapah Road, Perak, Malaysia.
[3] Malaysian Research Institute on Ageing (MyAgeing®), Universiti Putra Malaysia, Selangor, Malaysia.
[4] Pluripotent Stem Cell Laboratory, Haematology Unit, Cancer Research Centre, Institute for Medical Research (IMR), Block C, National Institute of Health (NIH) Malaysia, Setia Alam, Malaysia.
[5] Department of Human Anatomy, Faculty of Medicine and Health Sciences, University Putra Malaysia, 43400 Serdang, Selangor, Malaysia.
* Correspondence: lkh@upm.edu.my ; Tel.: +603-8947 2564

Received: 29 September 2025; **Accepted:** 7 June 2026; **Published:** 30 June 2026
Edited by: Narisorn Kitiyanant (Mahidol University, Thailand)
Reviewed by: Shahidee Zainal Abidin (Universiti Malaysia Terengganu, Malaysia);
Jambaldorj Jamiyansuren (Mongolian National University of Medical Sciences, Mongolia).
https://doi.org/10.31117/neuroscirn.v9i2.509

Abstract: RE1-silencing transcription factor (REST), a key regulator of neural gene expression, modulates ion channel function, neurotransmitter receptor activity, and synaptic plasticity, and its dysregulation has been implicated in neurodegenerative diseases. However, stable overexpression of REST in mammalian cells remains technically challenging, highlighting the need for an efficient and controllable delivery platform. Here, we constructed and validated a PiggyBac-based inducible vector system for regulatable REST overexpression in HEK293FT cells as a proof of concept. The REST-FLAG-P2A-GFP construct was assembled using NEBuilder HiFi DNA Assembly and validated by restriction fragment length polymorphism (RFLP), Sanger sequencing, and whole-plasmid sequencing. HEK293FT cells were transfected with REST-FLAG-P2A-GFP and SB100X, together with Xlone_GFP plasmids, using polyethylenimine (PEI), followed by doxycycline induction at 24 and 48 hours post-transfection. REST expression was confirmed by eGFP fluorescence imaging, while blasticidin resistance supported stable transgene integration for up to 5 days. Western blot analysis further verified inducible REST overexpression, detecting REST protein at approximately 130 and 200 kDa, with 1.45-fold ($p < 0.01$) and 1.56-fold ($p < 0.05$) increases, respectively, compared with uninduced cells. Collectively, these findings demonstrate the utility of the PiggyBac transposon system for stable and inducible expression of transcription factors in mammalian cells and establish a platform for future studies of REST function and gene regulatory mechanisms.

Keywords: PiggyBac; RE1-Silencing Transcription Factor (REST); Molecular cloning; Transfection.

1.0 INTRODUCTION

Genetic engineering is widely used to study gene function by applying gain-of-function or loss-of-function modifications. A common approach involves utilising vector systems to induce or suppress the expression of specific genes, thereby producing proteins such as transcription factors, enzymes, and growth factors, as well as microRNAs. Gene delivery methods include both viral and non-viral approaches, each presenting unique advantages and challenges. While viral vectors are efficient, they raise concerns regarding safety and ethics. In contrast, plasmid-based non-viral vectors often suffer from low transfection efficiency and poor genomic integration rates (Chen et al., 2018; Hackett et al., 2010). Moreover, plasmid-based expression systems often lead to random gene integration, resulting in inconsistent recombinant protein expression (Matasci et al., 2011).

To overcome these limitations, transposon-based vector systems have emerged as powerful non-viral tools for stable gene integration in mammalian cells. Among the best-characterised DNA transposon platforms are PiggyBac (PB) and Sleeping Beauty (SB), both of which operate through a "cut-and-paste" mechanism in which a transposase enzyme recognises terminal repeat sequences flanking the transgene cassette, excises the cassette from the donor plasmid, and catalyses its integration into the host genome (Hackett et al., 2010; Ivics et al., 2009; Wu et al., 2006). Although both systems support long-term genomic insertion, they differ in several important molecular features. PB integrates preferentially at TTAA tetranucleotide sites and can excise precisely without leaving a footprint, which is advantageous for reversible engineering and for delivery of relatively large cargos. In contrast, SB integrates primarily into TA dinucleotides and has been widely used for stable transgenesis and gene transfer in vertebrate cells (Ivics et al., 2009; Li et al., 2013; Wu et al., 2006). In mammalian systems, piggyBac has frequently demonstrated high transposition activity and the ability to accommodate relatively large transgene cargos, making it useful for delivering complex expression cassettes (Lacoste et al., 2009; Wilson et al., 2007; Wu et al., 2006; Zhao et al., 2016).

A major advantage of PB- and SB-based systems is that genomic integration can be achieved using a simple binary configuration in which the donor vector carries the transgene of interest between terminal repeats. At the same time, the transposase is supplied in trans. This design reduces persistent remobilisation once transposase expression ceases and supports relatively stable, long-term transgene expression after integration (Hackett et al., 2010; Ivics et al., 2009; Mátés et al., 2009). Compared with conventional plasmid transfection, which is often transient and prone to silencing or variable expression, transposon-mediated integration improves the likelihood of sustained expression across cell divisions. These features are especially valuable for genes such as REST, whose large coding sequence and strong transcriptional regulatory activity make robust but controllable expression technically challenging.

In addition to transposon-based systems, other genome-engineering approaches have been developed to achieve stable transgene insertion, particularly when more precise genomic targeting is required. Among these, CRISPR/Cas9-based systems have emerged as powerful tools for locus-specific genome editing. However, conventional knock-in strategies rely on DNA cleavage and endogenous repair pathways, and their efficiency varies across cell types, donor designs, cargo sizes, and genomic contexts. Thus, despite recent advances, CRISPR-based insertion remains more technically complex than transposon-based integration, making a transposon-based inducible system a practical choice for proof-of-concept studies focused on durable, regulatable overexpression rather than precise locus targeting (Doudna & Charpentier, 2014; Fong & Ceroni, 2025; Gwon et al., 2025; Hsu et al., 2014).

Beyond the choice of integration strategy, the design of the inducible plasmid system was also an important consideration in the present study. The expression cassette was designed to enable controlled REST induction via a Tet-On-regulated system, visual monitoring of transgene expression via GFP, and enrichment of stable integrants through antibiotic selection. This inducible configuration was intended to provide controlled, traceable, and sustained REST overexpression in a proof-of-concept mammalian cell

platform before future application in more biologically relevant models.

REST is a key regulator of neuronal gene expression and is critically involved in synaptic plasticity, neurotransmitter receptor expression, and ion channel function (Chong et al., 1995; Lim et al., 2025). Dysregulation of REST has been implicated in neurodegenerative diseases, including Alzheimer's disease (AD) and Down syndrome (DS), where loss of REST function leads to increased oxidative stress, apoptosis, and impaired neurogenesis (Lu et al., 2014; Meyer et al., 2019; Zhao et al., 2017). However, REST overexpression poses technical challenges due to its large size (3331 bp) and potential cytotoxic effects, as it represses numerous target genes. Additionally, because stable and regulatable REST overexpression is technically challenging, an experimentally tractable mammalian cell system was first required to validate transgene integration, inducibility, and expression control before the platform could be transferred to more disease-relevant neuronal models.

HEK293FT cells were selected as an experimentally tractable mammalian host for proof-of-concept validation of the inducible transposon system, rather than as a physiologically relevant neuronal model. This choice was based on the well-established utility of HEK293-derived cells for plasmid-based engineering and recombinant expression, owing to their high transfection efficiency, rapid growth, and robust support for transgene production (Tan et al., 2021). In contrast, more disease-relevant studies of REST would require neuronal models such as iPSC-derived neural cells or organoids.

Accordingly, the primary objective of the present study was to construct and validate a transposon-based inducible REST overexpression system as a proof-of-concept platform in mammalian cells. Specifically, we aimed to generate a Tet-On-regulated REST-FLAG-P2A-GFP construct capable of controlled induction, visual monitoring of expression, and enrichment of stably integrated cells. The specific research gap addressed by this work is the lack of a stable and regulatable REST overexpression platform that can first be validated in an experimentally accessible cell background and subsequently adapted to more physiologically relevant neuronal systems. In this way, the present study was intended not as a disease model, but as a foundational technical step that may facilitate future mechanistic studies of REST function in iPSC-based neuronal and organoid models relevant to neurodevelopmental and neurodegenerative disease research.

2.0 MATERIALS AND METHODS

2.1 Plasmid preparation and molecular cloning

This study was approved by the Institutional Biosafety Committee (IBC), Department of Biosafety, the Malaysian Ministry of Natural Resources and Environmental Sustainability, under reference number JBK (S) 600-3/1/135 (11). In this study, we selected the Xlone_GFP plasmid (6327 bp) (**Figure 1A**) as the backbone for molecular cloning. This plasmid was obtained from Xiaojun Lian via Addgene (plasmid #96930; RRID: Addgene_96930; https://n2t.net/addgene:96930) (Randolph et al., 2017). The backbone plasmid was purchased, cultured, and extracted using the PrimeWay Plasmid DNA Extraction Kit (1st Base, Singapore).

The plasmids were then subjected to double digestion with the restriction enzymes KpnI and SpeI (FastDigest, Thermo Scientific, USA), followed by alkaline phosphatase treatment (FastDigest, Thermo Scientific, USA) according to the manufacturer's instructions. Digestion and dephosphorylation were carried out simultaneously at 37°C for 10 minutes, followed by enzyme inactivation at 80°C for 20 minutes. The dephosphorylated and digested plasmid was analysed by gel electrophoresis, which confirmed the presence of two bands at 5599 bp and 728 bp. The 5599 bp band was excised from the gel to ensure high purity of the linearised plasmid, followed by purification using the PrimeWay Gel Extraction/PCR Purification Kit (1st Base, Singapore).

Molecular cloning in this study was performed using NEBuilder HiFi DNA Assembly (NEB, UK), following the manufacturer's recommended 4–6 fragments assembly protocol. A total of three fragments were inserted into the linearised plasmid. These DNA fragments included REST, an oligonucleotide containing FLAG and P2A, and eGFP (**Figure 1**). The primer sequences for each fragment were designed using the NEBuilder Assembly Tool (https://nebuilder.neb.com/#!/). Only the REST and eGFP fragments required primers (**Table 1**), which were amplified by PCR from pooled human cDNA samples and the Xlone_GFP plasmid, respectively. The PCR was conducted using Phusion High-Fidelity DNA Polymerase (HF Buffer) (NEB, UK) and subsequently purified.

The FLAG–P2A oligonucleotides (81 bp) (**Table 1**) were synthesised separately for both strands and annealed

using a touchdown thermal cycling programme. The reaction was initially denatured at 95.0°C for 2 minutes, followed by 80 cycles of stepwise temperature reduction from 95.0°C at 1.0°C per cycle, with a 15 seconds hold per cycle, and a final hold at 16.0°C for 10 seconds. The annealed product was purified using the PrimeWay Gel Extraction/PCR Purification Kit (1st Base, Singapore) prior to dephosphorylation and assembly. The molar ratio for each of the three DNA fragments was calculated to be at least 0.2 pmol per fragment. The specific molar ratios used are shown in **Table 1**. The assembly reaction was carried out at 50°C for 60 minutes.

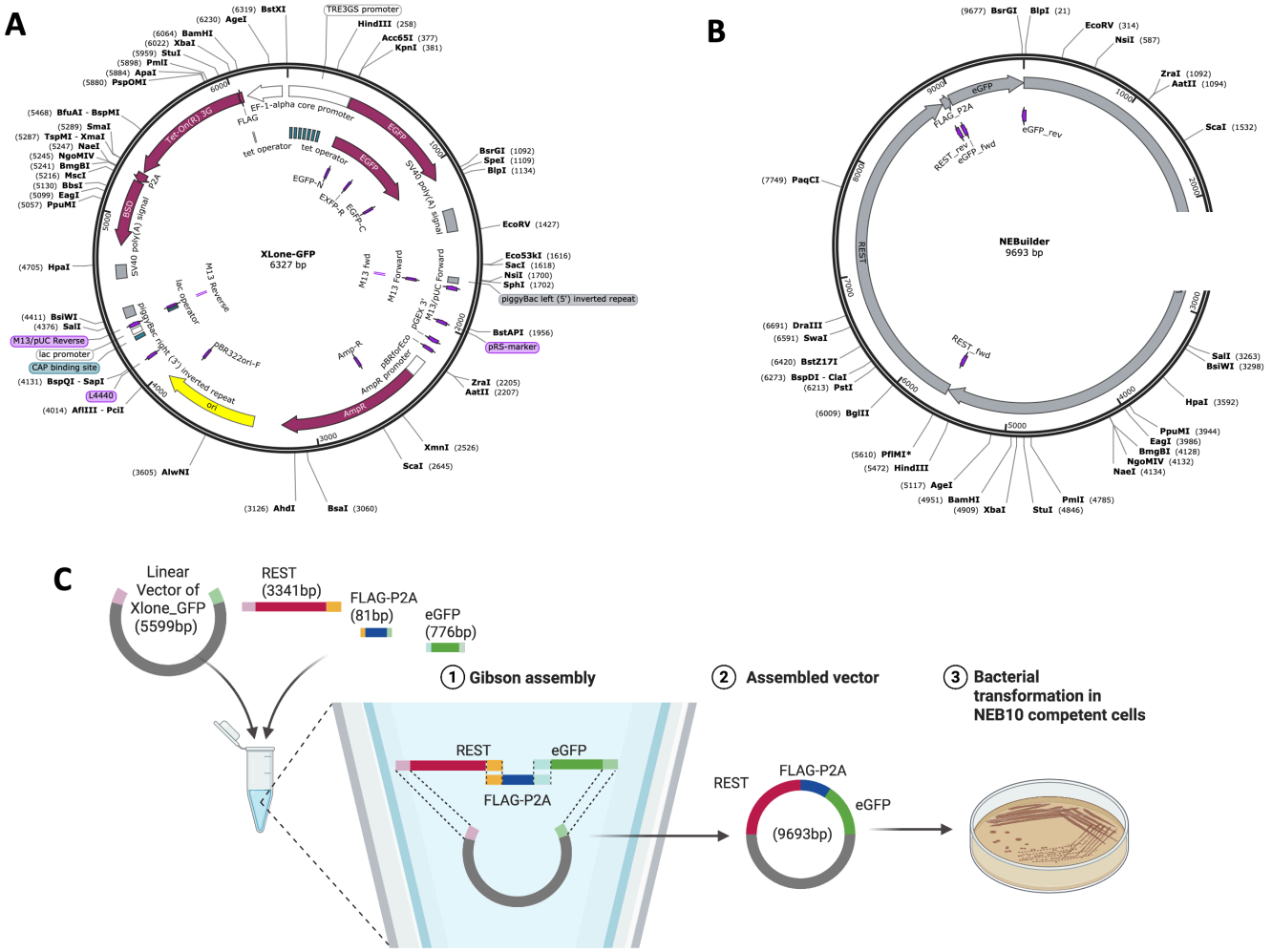

Figure 1. (A) Plasmid backbone Xlone_GFP from Addgene. (B) Generation of the Xlone_REST_FLAG_P2A_GFP plasmid via the NEBuilder assembly method (NEB, UK). (C) Diagrammatic representation of assembly of inserts into Xlone_GFP vector (Created in https://BioRender.com).

Table 1. Primers and molar ratios used for each insert DNA fragment. The required DNA mass for each fragment was calculated from fragment length and concentration using the NEBuilder assembly tool, with each fragment adjusted to at least 0.2 pmol to maintain an appropriate molar ratio for efficient multi-fragment assembly.

Fragment (bp)	Production	Primers (5'→3')	Molar ratio (Ratio to vector)
REST (3341 bp)	PCR	F: CCACTTCCTACCCTCGTAAAGGTACATGGCCACCCAGGTAATG R: CCTTGTCGTCATCGTCTTTGTAGTCCTCCTGCCCTTGAGCTGC	1.5
FLAG-P2A (81 bp)	Synthesis, annealing and PCR	GACTACAAAGACGATGACGACAAGGCCACTAACTTCTCCCTGTTGAAACAAGCA GGGGATGTCGAAGAGAATCCCGGGCCA	10
GFP (776 bp)	PCR	F: GGATGTCGAAGAGAATCCCGGGCCAATGGTGAGCAAGGGCGAG R: CTTAGCTCGCAGGGGAGGTGGTCTATTAGAATTCCTTGTACAGCTCG	5

2.2 Transformation and screening

Competent NEB10 beta cells were prepared by expanding bacterial cultures and washing the cell pellet with cold 100 mM $CaCl_2$ and cold 100 mM $MgCl_2$, followed by cryopreservation in cold 80 mM $CaCl_2$ with 15% glycerol. A total of 2 µl of the assembly reaction was added to 50 µl of in-house competent NEB10 beta cells, and the mixture was gently mixed by flicking three times. The mixture was then incubated on ice for 30 minutes, heat-shocked at 42°C for 30 seconds and incubated on ice for 5 minutes. Pre-warmed SOC media (950 µl) was added, and the mixture was incubated at 37°C for 1.5 hours with shaking (650 rpm).

Subsequently, 250 µl of the transformed mixture was spread on LB agar (BD Difco, USA) containing 100 µg/ml ampicillin and incubated at 37°C for 18 hours. Bacterial colonies were then picked, transferred into LB broth (BD Difco, USA) containing 100 µg/ml ampicillin, and cultured overnight (18 hours) in an incubator shaker at 37 °C (230 rpm). A positive control of the NEB HiFi Assembly Kit was also included to confirm colony formation.

Plasmid extraction and purification were performed using the PrimeWay Plasmid DNA Extraction Kit (1st Base, Singapore) following the manufacturer's instructions. Each purified transformant plasmid was further validated by comparing its size to that of the uncut vector using Restriction Fragment Length Polymorphism (RFLP) analysis. Only transformants with a larger plasmid size than the uncut vector were further analysed by RFLP. The RFLP was performed using single digestion with BamHI alone or double digestion with both BamHI and BglII in 1X NEBuffer 3.1 (NEB, UK), following the manufacturer's instructions (**Figure 1B**). Digestion of restriction enzymes was performed at 37°C for 60 minutes, followed by enzyme inactivation at 65°C for 20 minutes. The qualitative RFLP analysis was performed by electrophoresis on a prestained agarose gel with ViSafe Red Gel Stain (Vivantis Technologies, Malaysia). Clones yielding an approximately 1,000 bp DNA fragment were selected for further validation because this size was consistent with the expected colony PCR product of the recombinant construct. Accordingly, the ~1,000 bp band served as a preliminary indicator of successful insert incorporation before additional validation by Sanger sequencing of the FLAG-P2A oligonucleotide orientation.

2.3 DNA sequencing

Positive clones were confirmed by direct sequencing. Plasmids of the correct size were sequenced to verify the cloned sequences. Sanger sequencing was performed using five primer pairs at 1st BASE Laboratories Sdn Bhd. A total of 5 primer pairs were used, as follows: (First-Forward: CACTTCCTACCCTCGTAAAG and Reverse: GATGAGTCTTCTGAGAACTTG; Second-Forward: CCTTACTCAAGTTCTCAGAAG and Reverse: GAGCAGATCCCTTCTCAAC; Third-Forward: CTCAGAAGGAACCTGTTGAG and Reverse: CAAGTTTTGTCCAGAGGATG; Fourth-Forward: CCCATATTTCATCCTCTGG and Reverse: CGTCCTTGAAGAAGATGG; Fifth-Forward: GCACCATCTTCTTCAAGGAC and Reverse: CGCCTGTCTTAGGTTGGAG). To assess sequence specificity and detect any potential PCR-induced mutations, the generated sequences were aligned with reference sequences using Unipro UGENE 47.0 (Golosova et al., 2014; Okonechnikov et al., 2012; Rose et al., 2019). Each primer sequence was analysed against the original sequence of our construct using the NEBuilder Assembly Tool.

2.4 Cell culture and transfection

For the transfection experiments, HEK293FT cells were divided into four groups based on the plasmid combinations and induction conditions used. Group 1 served as the negative control and received the Xlone_GFP plasmid without doxycycline induction. Group 2 received the Xlone_GFP plasmid with doxycycline induction. Group 3 received the Xlone_REST_Flag_P2A_GFP plasmid without doxycycline induction, and Group 4 received the Xlone_REST_Flag_P2A_GFP plasmid with doxycycline induction. HEK293FT cells were maintained in a 5% CO_2 incubator at 37°C in DMEM (Gibco, USA) supplemented with 2 mM L-glutamine (Gibco, USA), 1 mM sodium pyruvate (Gibco, USA), 1X MEM Non-Essential Amino Acids (Gibco, USA), 100 U/ml penicillin/streptomycin, and 10% (v/v) fetal bovine serum (FBS).

All plasmids used for transfection were extracted using the ZymoPURE™ Plasmid Miniprep Kit (Zymo Research, USA) to obtain plasmid DNA with minimal endotoxin contamination. A total of 2.5 µg of plasmids, including the Xlone_REST_Flag_P2A_GFP or Xlone_GFP (positive control) and the transposase plasmid (SB100X) at a 5:1 ratio, were transfected into HEK293FT cells in suspension using Polyethylenimine (PEI) (Sigma, USA) at 1 mg/mL. A 1:3 plasmid-to-PEI volume ratio was used for transfection.

The plasmids and PEI were thoroughly mixed in OptiMEM medium (Gibco, USA) by gently pipetting up

and down, then incubated for 15–20 minutes before being added to the cell suspension. The suspension cells were mixed with full media supplemented with 5% FBS and 0.5% penicillin/streptomycin. The transfected cells were induced with doxycycline (1000 ng/mL) at 24 hours post-transfection to activate transgene expression through the Tet-On (rtTA/TRE) promoter system. eGFP expression was monitored at 24 hours and 48 hours after induction, corresponding to 48 hours and 72 hours post-transfection, respectively, using a JuLI™ Stage (NanoEnTek Inc., USA).

After 72 hours of transfection, the transfected cells were selected using blasticidin (8–9 µg/ml) for 5–7 days. Following antibiotic selection, the cells were re-induced with doxycycline for 48 hours before being harvested for protein extraction.

2.5 FACS analysis and cell sorting

After several passages, GFP+ cells were manually selected under a microscope as the number of non-GFP cells decreased. The cells were then analysed by flow cytometry to determine the percentage of GFP+ cells, comparing the Xlone_REST_Flag_P2A_GFP clone plasmid to the Xlone_GFP plasmid (positive control).

The GFP+ cells were further expanded and subjected to FACS analysis and sorting using the BD FACSAria Fusion Flow Cytometer (BD, USA). The number of cells for sorting was calculated based on the maximum cell count compatible with a 70 µm nozzle. GFP+ cells were sorted until approximately 300,000 cells were obtained in a single tube. The sorted cells were then washed twice with fresh complete media before being cultured in a 12-well plate.

2.6 Protein extraction, Western blot, and band intensity analysis

Cell pellets were washed twice with cold PBS and subjected to protein extraction using RIPA buffer (Thermo Fisher Scientific, USA) supplemented with 1X phosphatase inhibitor PhosSTOP™ (Roche, USA) and protease inhibitor (Thermo Scientific, USA). The mixture was resuspended multiple times, incubated on ice for 30 minutes, and centrifuged at 13,400 rpm for 30 minutes at 4°C. Protein concentration was quantified using the BCA Protein Assay Kit (Thermo Fisher Scientific, USA).

A total of 20 µg of protein was mixed with Laemmli buffer (Bio-Rad) containing 10% 2-mercaptoethanol, denatured at 100°C for 5 minutes, and loaded onto 4–20% Mini-PROTEAN TGX precast gels (Bio-Rad) for SDS-PAGE, run at 80 V for 10 minutes followed by 150 V for 30 minutes. Proteins from the gel were transferred to PVDF membranes using the Trans-Blot® Turbo™ Transfer System (#1704150; Bio-Rad, US) at the high-molecular-weight setting (10 minutes, 2.5 A). Membranes were stained with Ponceau S (5 minutes) to visualise protein bands, rinsed twice with TBST (5 minutes each), and blocked with 5% non-fat dry milk in Tris-buffered saline with 0.1% Tween 20 (TBST) for one hour at room temperature. Primary antibodies diluted in TBST with 2.5% non-fat milk were incubated overnight (16–18 hours) at 4°C on a shaker at 30 rpm, followed by three TBST washes (5 minutes each) and a 1-hour incubation with HRP-conjugated secondary antibodies at room temperature. The primary and secondary antibodies used for the Western blot are listed in **Table 2**. After three additional TBST washes, a chemiluminescent substrate was applied for 5 minutes, and the signals were detected using the G: BOX gel documentation system (Synoptics Ltd, UK). Band intensity was measured using ImageJ software (Fiji version 2.16.0/1.54p).

2.7 Statistical analysis

Statistical analyses were conducted using GraphPad Prism 9.0. Data are presented as mean ± standard deviation (SD) from four biological replicates. Comparisons between two groups were performed using a one-tailed Student's *t*-test. Differences were considered statistically significant at $*p<0.05$ and $p<0.01$, whereas *ns* indicated no significant difference.

Table 2. List of primary and secondary antibodies for Western blot.

Protein name	Brand (Country)	Catalogue no.	Dilution	Host
REST	Proteintech (USA)	22242-1-AP	1:1000	Rabbit
GFP	Millipore (Germany)	AB3080	1:1000	Rabbit
FLAG	Elabscience (China)	E-AB-20006	1:1000	Mouse
Beta actin	Elabscience (China)	E-AB-40338-120uL	1:10000	Rabbit
Goat Anti-Mouse IgG H&L (HRP)	Abcam (USA)	AB6789	1:4000	Mouse
Goat Anti-Rabbit IgG H&L (HRP)	Abcam (USA)	AB6721	1:4000	Rabbit

3.0 RESULTS AND DISCUSSION

In this study, we successfully constructed and validated a doxycycline-inducible RE1-silencing transcription factor (REST) overexpression system using a PiggyBac (PB)-based transposon vector. This platform enabled stable genomic integration and inducible expression in mammalian cells, offering advantages over conventional transient plasmid transfection, particularly for large and transcriptionally repressive genes such as REST. The PB system was used in a binary configuration, in which the transposon and transposase were delivered separately to promote efficient genomic integration. Compared with viral vectors, PB-based systems are safer, more scalable, and capable of carrying relatively large DNA inserts while maintaining high transposition efficiency (Li et al., 2013; Wilber et al., 2007; Zhao et al., 2016). More broadly, both PiggyBac and Sleeping Beauty are well-established non-viral transposon platforms for stable genomic integration and sustained transgene expression in mammalian cells, supporting the use of transposon-based engineering to establish an inducible REST overexpression model (Nakazawa et al., 2013; Sandoval-Villegas et al., 2021; Turchiano et al., 2014).

To generate the recombinant construct, we employed NEBuilder HiFi DNA Assembly (NEB, UK), a Gibson assembly-derived approach suitable for seamless multi-fragment cloning. Prior *in silico* simulation using the manufacturer's design platform predicted a final construct size of 9693 bp (**Figure 1A** and **Figure 1B**) and guided the design of fragment-specific primers with appropriate overlapping extensions. The original eGFP cassette was first removed to permit reconstruction of the expression cassette into the required REST-FLAG-P2A-GFP configuration, after which eGFP was reintroduced to preserve its role as a fluorescent reporter. Thus, rather than performing a simple direct insertion of REST using ACC65I/KpnI, the vector was redesigned stepwise to achieve the desired architecture for regulated expression and downstream visualisation.

The FLAG-P2A sequence was incorporated to support both protein detection and reporter-based monitoring of transgene expression. Specifically, the FLAG epitope enabled immunological detection of recombinant REST, whereas the P2A peptide mediated co-expression of REST and GFP from a single open reading frame via ribosomal skipping during translation (Donnelly et al., 2001; Kim et al., 2011). This arrangement allowed GFP fluorescence to serve as a visual readout of inducible transgene expression while REST protein expression could still be verified directly by immunoblotting. Because the FLAG-P2A fragment was short and sequence-defined, it was introduced using commercially synthesised oligonucleotides rather than template-based PCR amplification. This strategy simplified construct assembly and reduced opportunities for polymerase-associated sequence errors prior to final sequence verification, although synthetic DNA also requires validation, as synthesis-derived errors may occur (Hughes & Ellington, 2017; McInerney et al., 2014).

Primers were therefore generated only for the REST DNA fragment and eGFP, whereas the FLAG-P2A sequence was incorporated during construct assembly using synthesised oligonucleotides (**Figures 2C-i** to **iii**). During gel-based verification, the appearance of two eGFP bands may reflect heteroduplex formation or minor nonspecific PCR products, both of which have been reported to generate additional bands on agarose gels (Thompson et al., 2002). Nevertheless, the expected eGFP amplicon was present and considered suitable for downstream assembly. The restriction sites present in the original plasmid backbone were not retained in the final recombinant construct after cloning and assembly, most likely because cassette reconstruction altered the local sequence context, eliminating previously available recognition sites. Similar loss or replacement of restriction sites has been described in recombination-based DNA assembly and construct refactoring workflows, in which local sequence redesign can delete or substitute pre-existing sites (Kalva et al., 2018). Consequently, alternative restriction enzymes were selected for RFLP analysis based on the updated final construct sequence.

Transformation of NEB 10-beta competent cells yielded only a limited number of colonies. Across four plates, only 10 unique colonies were obtained, suggesting that the multi-fragment assembly reduced overall cloning efficiency. Of these, nine colonies were selected for plasmid size verification and RFLP analysis. Four transformants exhibited larger plasmid sizes than the control vectors (**Figure 2B-i** and **Figure 2B-ii**), consistent with successful incorporation of the intended insert. These four clones were then analysed by RFLP using double digestion with BamHI and BglII and single digestion with BamHI alone. All four displayed the expected fragment sizes of 1058 bp and 5599 bp, confirming correct insertion. In **Figure 2B-ii**, lane 2a, a faint additional band was observed below the 5599 bp fragment, suggesting partial or incomplete digestion.

Sanger sequencing was subsequently performed to verify the orientation of the FLAG-P2A oligonucleotide in all four positive clones. Full sequencing was then carried out for clones 8 and 9, and the complete recombinant vector sequence was confirmed by pairwise alignment with the reference construct using UGENE software. Clone 8 (**Figure 2B-iii**, lanes 8a and 8b) showed the expected validation pattern and was therefore selected for functional testing in HEK293FT cells. Rather than serving as a model of neurodegeneration, HEK293FT cells were used in this study as a technically convenient mammalian platform for initial construct validation. This choice was supported by the well-established use of HEK293-derived cells for high-efficiency transfection, heterologous protein expression, and rapid experimental optimisation. In contrast, more biologically relevant studies of REST in neurodegeneration would require neuronal systems such as iPSC-derived neurons or organoids.

The validated vector was transfected into HEK293FT cells to assess inducible expression. Mock-transfected HEK293FT cells and cells transfected with Xlone_GFP were included as negative and positive controls, respectively. The mock control showed no background autofluorescence or nonspecific GFP signal. In contrast,

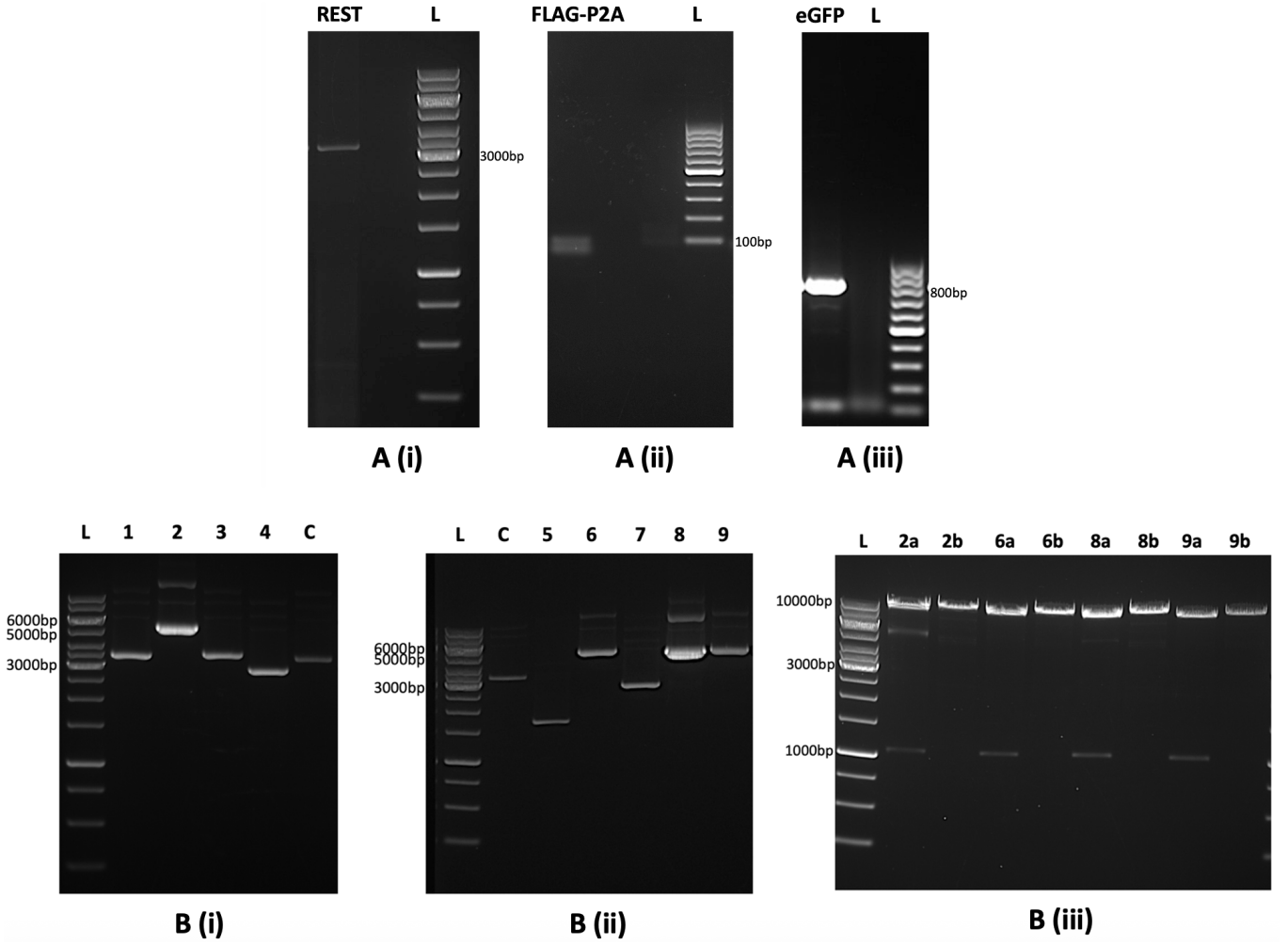

Figure 2. Before assembly, (A-i) the REST, (A-ii) FLAG-P2A, and (A-iii) eGFP were amplified by PCR. After cloning (B-i to ii), a total of nine bacterial colonies (i–Lanes 1–4; ii–Lanes 5–9) were picked, cultured, and plasmids were extracted to verify their sizes against the plasmid control (Xlone_GFP) (B-i–Lane C and B-ii–Lane C). RFLP analysis was performed to confirm plasmid sizes by digestion with the restriction enzymes BamHI and BglII, yielding ~1000 bp and 5599 bp fragments (B-iii). Single digestion with BamHI was performed. Lane 2a (double digestion) and 2b (single digestion) represent the first clone; Lane 6a (double digestion) and 6b (single digestion) represent the sixth clone; Lane 8a (double digestion) and 8b (single digestion) represent the eighth clone; and Lane 9a (double digestion) and 9b (single digestion) represent the ninth clone.

the Xlone_GFP construct served as a positive control to assess transfection efficiency and the proper functioning of the doxycycline-inducible system. At 48 and 72 hours post-transfection, following doxycycline induction at 24 and 48 hours, eGFP-positive cells were detected in both the Xlone_REST_FLAG_P2A_GFP and Xlone_GFP groups, but not in the mock control (**Figure 3**). These findings confirmed that the validated vectors were functional and capable of driving inducible reporter expression.

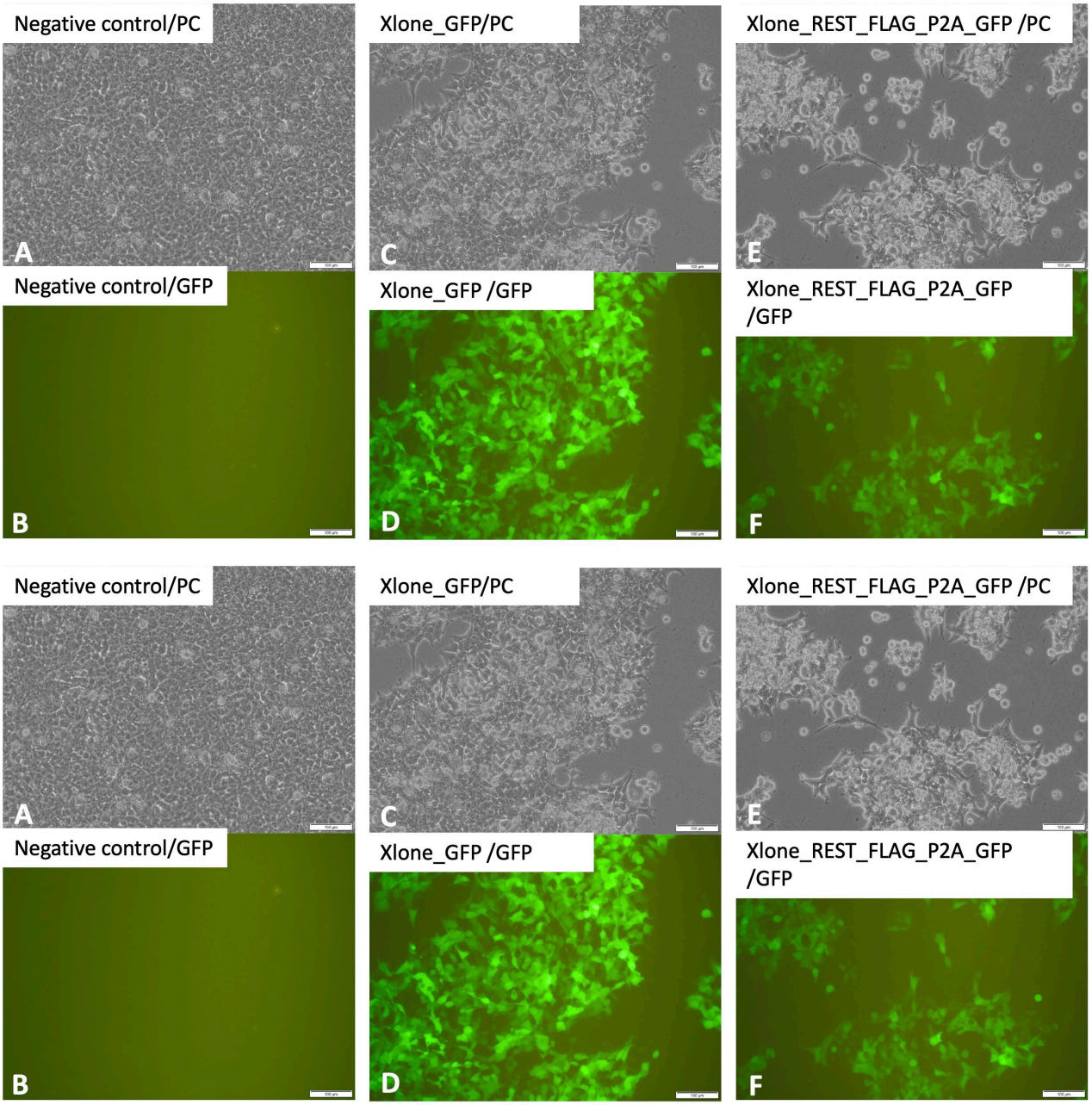

Figure 3. Transfection of HEK293FT cells with Xlone_GFP and Xlone_REST_FLAG_P2A_GFP expression vectors. At 24 hours post-transfection, the transfected cells, along with negative controls, were induced with 1 µg/ml doxycycline. The negative controls (A-B and G-H) were treated with only the transfection mixture, without any vectors, and did not express eGFP. Phase contrast (PC) and fluorescence images were captured 24 hours (A-F) and 48 hours (G-L) after doxycycline induction. Cells transfected with Xlone_REST_FLAG_P2A_GFP displayed dimmer eGFP fluorescence compared to those transfected with Xlone_GFP. The scale bar is 100 µm.

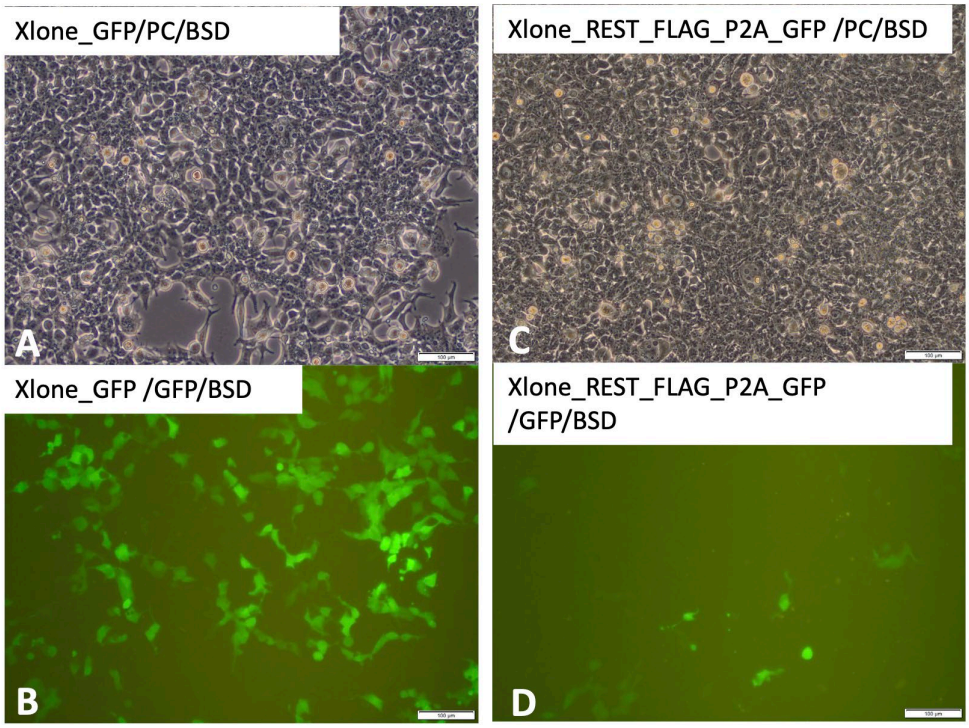

Figure 4. Transfected HEK293FT cells with constructed expression vectors of Xlone_GFP and Xlone_REST_FLAG_P2A_GFP after blasticidin (BSD) selection. At 48 hours post-doxycycline (1 ug/ml), phase contrast (PC) and fluorescence images were taken. Cells with Xlone_REST_FLAG_P2A_GFP show less eGFP compared to cells with Xlone_GFP. The scale bar is 100 µm.

Incorporation of the eGFP reporter enabled straightforward visual monitoring of transgene expression. Detection of eGFP fluorescence indicated successful co-expression of the downstream reporter, consistent with the high cleavage efficiency reported for 2A peptides in mammalian systems (Donnelly et al., 2001; Kim et al., 2011). However, fluorescence intensity differed between the GFP control and REST_FLAG_P2A_GFP groups, suggesting differences in transgene output and/or cellular tolerance to REST overexpression. Although doxycycline induction clearly produced eGFP-positive cells, both fluorescence intensity and uniformity decreased after blasticidin selection and subsequent passaging. Rather than simply reflecting persistence of non-transfected cells, this reduction more likely indicates heterogeneity in stable transgene expression and/or partial silencing following genomic integration. These phenomena have been described in antibiotic-selected cell populations and are influenced by local chromatin context and position effects (Kaufman et al., 2008). In addition, transcription factor overexpression can alter cellular fitness and transcriptomic state (Parekh et al., 2018), potentially favouring the survival of cells with lower REST_FLAG_P2A_GFP expression.

The decline in eGFP expression is also consistent with previous reports of transgene silencing or variegated expression due to epigenetic modifications, positional effects, or cell-cycle-dependent regulation (Kaufman et al., 2008). REST overexpression itself may have contributed to this phenotype. REST has been associated with suppression of epithelial cell growth, tumour-suppressive activity, mitochondrial dysfunction, reduced dendritic spine density, and apoptosis in different cellular contexts (Indo et al., 2024; Liu et al., 2022). Blasticidin selection may therefore have enriched for cells with lower transgene output, reflecting REST-dependent effects on stress response, survival, and cell state. The reduced eGFP intensity and altered morphology observed here may also be attributable to REST-mediated transcriptional repression or epigenetic silencing of the integrated transgene. REST has been reported to influence chromatin accessibility and methylation status, thereby modulating the expression of genes involved in differentiation and extracellular matrix remodelling (Perycz et al., 2024).

Flow cytometry analysis (**Figure 5**) further confirmed the presence of eGFP-positive cells in both the GFP control and REST_FLAG_P2A_GFP-transfected HEK293FT populations. However, both the percentage

of GFP-positive cells and the mean fluorescence intensity (MFI) were higher in control eGFP cells than in REST_FLAG_P2A_GFP cells, indicating reduced reporter output in the presence of REST overexpression. After sorting (**Figure 6**), GFP-positive populations were enriched and successfully expanded. Fluorescence imaging at 48 hours post-doxycycline induction showed that REST_FLAG_P2A_GFP-transfected cells retained eGFP expression, albeit at a lower intensity than the GFP control, consistent with the microscopy and flow cytometry findings.

Western blot analysis validated REST overexpression (**Figure 7**), detecting REST at approximately 200 kDa and 130 kDa in doxycycline-induced REST_FLAG_P2A_GFP cells. Quantification showed significant upregulation of REST protein, with a 1.56-fold increase (p<0.05) at ~200 kDa and a 1.45-fold increase (p<0.01) at ~130 kDa in induced cells relative to non-induced controls. In contrast, eGFP control cells showed no detectable change. Because HEK293-derived cells express endogenous REST, this system should be interpreted as an inducible REST overexpression model on top of a basal endogenous background rather than as a *de novo* REST expression system (Cavadas et al., 2015). Accordingly, the increased REST bands observed following doxycycline treatment reflect augmentation of pre-existing cellular REST levels rather than the emergence of REST expression in a previously REST-null background. This interpretation is important because it indicates that the observed phenotype arose from increased REST dosage within an existing regulatory network, rather than from the initial introduction of REST into a REST-negative host.

These findings confirm that the construct functioned as intended after doxycycline induction. However, the reduced eGFP intensity in REST-overexpressing cells suggests an interaction between exogenous REST expression and endogenous host-cell regulatory pathways. As a master regulator of neuronal gene expression, REST participates in chromatin remodelling and transcriptional repression (Ballas et al., 2005). Its overexpression may therefore perturb broader gene networks linked to differentiation, metabolism, cellular stress, and survival. Because eGFP was expressed from the same inducible cassette, such perturbations may also have indirectly affected reporter expression, contributing to variability in fluorescence intensity and reduced cell viability. These observations are consistent with previous reports linking REST to suppression of proliferation and promotion of apoptosis in both epithelial and neuronal cells (Indo et al., 2024; Liu et al., 2022).

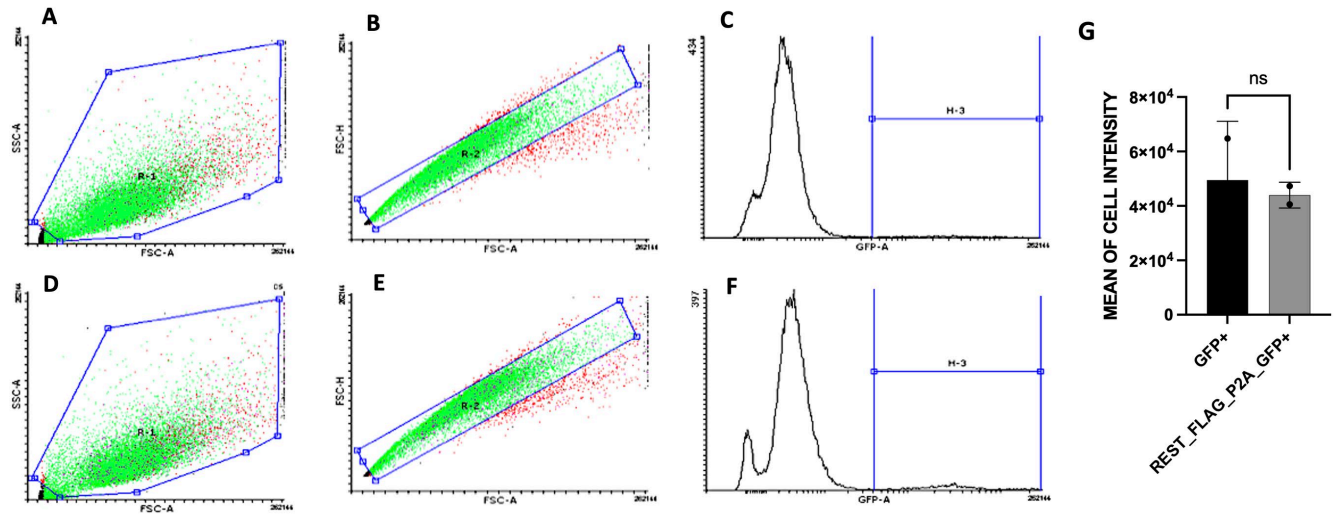

Figure 5. Flow cytometry (FACS) analysis of GFP+ cells before sorting. (A–C) Representative gating strategy for control GFP+ cells: (A) Forward scatter area (FSC-A) versus side scatter area (SSC-A) to define the main cell population, (B) FSC-A versus forward scatter height (FSC-H) to exclude doublets, and (C) GFP fluorescence intensity histogram (H-3 gate) showing the GFP+ population. (D–F) Representative gating strategy for REST_FLAG_P2A_GFP+ cells using the same sequential steps: (D) FSC-A versus SSC-A, (E) FSC-A versus FSC-H, and (F) GFP fluorescence intensity histogram identifying the GFP+ population. (G) Mean fluorescence intensity (MFI) of GFP+ cells for both groups before sorting, indicating relative GFP expression levels. This analysis was performed to assess the abundance and fluorescence intensity of GFP+ cells prior to sorting, to ensure optimal gating parameters and maximise sorting efficiency. Data are presented as mean ± SD from two independent experiments.

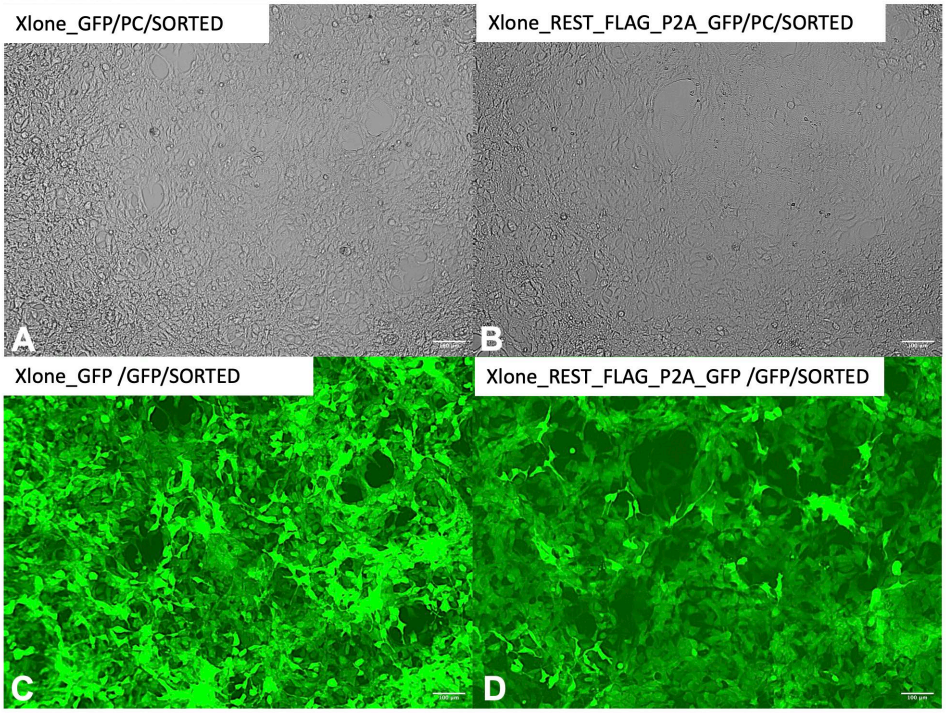

Figure 6. (A, C) Sorted, transfected HEK293FT cells with the control plasmid Xlone_GFP, shown in phase-contrast (PC) and GFP channels, respectively. (B, D) Sorted transfected HEK293FT cells with the constructed expression vector Xlone_REST_FLAG_P2A_GFP, shown in PC and GFP channels, respectively. Images were acquired 48 hours after doxycycline induction (1 µg/mL). Scale bar: 100 µm.

In addition to REST's direct effects, newly integrated foreign DNA can be silenced by endogenous chromatin-silencing complexes such as HUSH, which initiate heterochromatin formation and suppress foreign promoters independently of REST activity, thereby reducing fluorescent reporter expression (Lehner, 2025). Such mechanisms may act synergistically with REST's repressive functions, explaining the dim GFP fluorescence and cellular stress observed in this study.

Although FLAG-tagged REST was detected at approximately 130 kDa and 200 kDa, the FLAG signals were relatively weak. Detection of the FLAG epitope depends on antibody specificity and tag accessibility. The FLAG tag is widely used because it is short, hydrophilic, and readily recognised by anti-FLAG monoclonal antibodies, making it suitable for detecting recombinant proteins (Knappik & Plückthun, 1994). However, signal intensity can be influenced by tag position, protein folding, and post-translational modification. For example, some anti-FLAG antibodies recognise only N-terminal FLAG epitopes, whereas others detect FLAG irrespective of position. Moreover, tyrosine sulfation has been reported to hinder FLAG recognition and reduce signal intensity, particularly for antibodies that are more sensitive to this modification (Guo et al., 2021; Hunter et al., 2016; Schmidt et al., 2012). These factors may have contributed to the comparatively weak FLAG immunoblot signal observed here.

Additional FLAG-reactive bands were also detected at approximately 35–42 kDa in doxycycline-treated samples (**Figure 7**). REST undergoes alternative splicing, generating multiple transcript variants that encode distinct protein isoforms (Chen & Miller, 2013). Different anti-REST antibodies can therefore yield distinct immunoblot patterns, reflecting the structural and functional diversity of REST isoforms (Chen & Miller, 2018). Furthermore, REST isoforms often migrate at molecular weights that differ from their predicted values due to post-translational modifications. For example, REST4 and RESTC, predicted at 37 kDa and 86 kDa, respectively, have been detected at approximately 53 kDa and 130 kDa on Western blot, whereas full-length REST has been reported across a broad range of ~120–200 kDa (Lee et al., 2000; Nechiporuk et al., 2016; Zhang et al., 2011). This complexity in isoform structure and post-translational processing likely accounts for the unexpected FLAG-associated bands observed in the present study.

Overall, despite the transient and somewhat heterogeneous nature of REST overexpression, these

findings demonstrate the utility of the PiggyBac system as a robust non-viral gene delivery platform for inducible mammalian expression studies. Compared with conventional plasmid transfection, transposon-mediated integration supports longer-term transgene maintenance and more sustained expression in mammalian cells (Nakazawa et al., 2013; Sandoval-Villegas et al., 2021). At the same time, the present findings highlight important biological and technical constraints, including endogenous REST background, position-effect variegation, epigenetic silencing, and possible selection against cells with high REST expression. An additional limitation of this study is that the efficiency of the PiggyBac transposon system was not directly compared with other viral or non-viral delivery platforms, such as lentiviral vectors, conventional plasmid transfection, or alternative transposon systems. Therefore, although the present data support the functionality of PiggyBac for inducible REST overexpression, they do not permit definitive conclusions regarding its relative efficiency, stability, or superiority over other available gene delivery approaches. Future refinements, such as incorporating chromatin insulators, alternative promoter configurations, using host cell systems with lower endogenous REST expression, and conducting direct side-by-side comparisons with other delivery systems, may improve the stability, uniformity, and interpretability of inducible REST overexpression in mammalian cells.

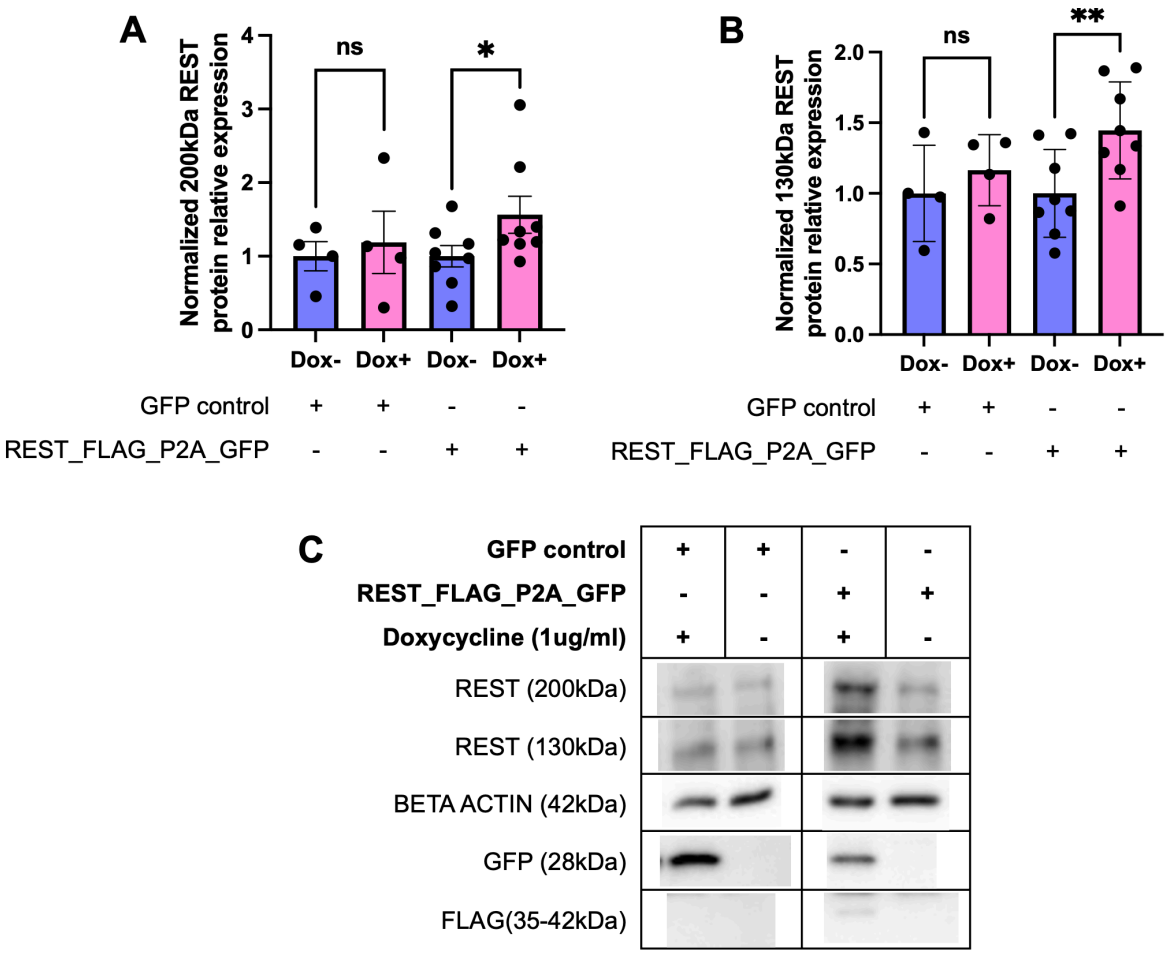

Figure 7. Analysis of REST protein expression in transfected GFP control or REST_FLAG_P2A_GFP HEK293FT cells. (A) and (B) Quantification of 200 kDa and 130 kDa protein relative expression, respectively, normalised to the average of the non-doxycycline-induced cells (Dox−). Data are presented as the mean with standard deviation (SD), along with individual data points. Statistical significance was determined using a one-tailed t-test, where *p<0.05, **p<0.01, and "ns" indicates non-significance. (C) Representative Western blot images showing REST expression at 200 kDa and 130 kDa, along with loading controls β-Actin (42 kDa) and GFP (28 kDa). REST protein expression levels at 130 kDa and 200 kDa were significantly different in Dox+ REST_FLAG_P2A_GFP cells as compared to the Dox- (C). In contrast, no significant difference was observed in the expression of REST (200 kDa and 130 kDa) in Dox+/Dox- GFP control cells. GFP expression was detected in both GFP control and REST_FLAG_P2A_GFP cells in the presence of doxycycline. FLAG expression at (35-42 kDa) was detected only in REST_FLAG_P2A_GFP cells in the presence of doxycycline.

4.0 CONCLUSIONS

In conclusion, this study successfully established and validated a doxycycline-inducible REST overexpression system based on the PiggyBac transposon platform in HEK293FT cells. The REST-FLAG-P2A-GFP construct was successfully assembled, sequence-verified, and functionally expressed following doxycycline induction. eGFP fluorescence, flow cytometry, and Western blotting consistently confirmed inducible transgene expression, while increased REST protein levels at approximately 200 and 130 kDa demonstrated successful overexpression above the endogenous basal REST background. At the same time, the reduced eGFP intensity observed after selection and passaging indicated heterogeneity in stable expression and suggested that REST overexpression may affect cellular fitness, reporter output, and transgene stability. Collectively, these findings demonstrate that the PiggyBac system is a useful non-viral platform for inducible REST expression in mammalian cells, while also highlighting important technical and biological constraints to consider when interpreting overexpression-based models. Future work in more disease-relevant neuronal systems may further clarify the role of REST in neurodevelopmental and neurodegenerative disorders.

Supplementary Materials: The following are available online at https://neuroscirn.org/ojs/index.php/nrnotes/article/view/509; **Figure S1**: SBSleeping Beauty (SB100X) plasmid as the transposase. **Figure S2**: Sanger sequencing validation of key cloned regions in the REST-FLAG-P2A-GFP recombinant construct. (A) Representative Sanger sequencing chromatogram showing the FLAG-P2A region of the recombinant construct. The sequence spanning approximately 8887 bp to 8967 bp confirms the expected nucleotide composition across the inserted FLAG tag and P2A peptide region. Dashed lines indicate the validated boundaries of the sequenced segment. (B) Representative Sanger sequencing chromatogram showing the junction between the REST coding sequence and the beginning of the FLAG sequence. The sequence trace confirms the correct continuity, orientation, and in-frame fusion of REST with the downstream FLAG tag. Together, these chromatograms verify accurate assembly of the recombinant REST-FLAG-P2A-GFP construct at the key insertion and junction regions.

Acknowledgements: This work was supported by the Ministry of Higher Education under the Fundamental Research Grant Scheme (FRGS) (FRGS/1/2022/SKK10/UPM/02/4) awarded to K-HL.

Author Contributions: KHL, PSC, NN, and NJ conceived and designed the experiments; NJ and NANMY designed and performed the flow cytometry and cell sorting experiments; NJ and KHL analysed the data; NJ wrote the first draft of the manuscript; PSC, NN and KHL contributed to manuscript writing; NJ and KHL agreed with the manuscript results and conclusions and developed the paper's structure and arguments; NJ and KHL made critical revisions and approved the final version. All authors reviewed and approved the final manuscript.

Conflicts of Interest: The authors declare no conflict of interest.

References

Ballas, N., Grunseich, C., Lu, D. D., Speh, J. C., & Mandel, G. (2005). REST and its corepressors mediate plasticity of neuronal gene chromatin throughout neurogenesis. *Cell*, *121*(4), 645–657. https://doi.org/10.1016/j.cell.2005.03.013

Cavadas, M. A. S., Mesnieres, M., Crifo, B., Manresa, M. C., Selfridge, A. C., Keogh, C. E., Fabian, Z., Scholz, C. C., Nolan, K. A., Rocha, S., Tambuwala, M. M., Cummins, E. P., & Taylor, C. T. (2015). REST mediates resolution of HIF-dependent gene expression in prolonged hypoxia. *Scientific Reports*, *5*, 17851. https://doi.org/10.1038/srep17851

Chen, G. L., & Miller, G. M. (2013). Extensive alternative splicing of the repressor element silencing transcription factor linked to cancer. *PLoS ONE*, *8*(4), e62217. https://doi.org/10.1371/journal.pone.0062217

Chen, G. L., & Miller, G. M. (2018). Alternative REST splicing underappreciated. *ENeuro*, *5*(5), ENEURO.0034-18.2018. https://doi.org/10.1523/eneuro.0034-18.2018

Chen, Y. H., Keiser, M. S., & Davidson, B. L. (2018). Viral vectors for gene transfer. *Current Protocols in Mouse Biology*, *8*(4), e58. https://doi.org/10.1002/cpmo.58

Chong, J. A., Tapia-Ramirez, J., Kim, S., Toledo-Aral, J. J., Zheng, Y., Boutros, M. C., Altshuller, Y. M., Frohman, M. A., Kraner, S. D., & Mandel, G. (1995). REST: A mammalian silencer protein that restricts sodium channel gene expression to neurons. *Cell*, *80*(6), 949–957. https://doi.org/10.1016/0092-8674(95)90298-8

Donnelly, M. L. L., Hughes, L. E., Luke, G., Mendoza, H., Ten Dam, E., Gani, D., & Ryan, M. D. (2001). The "cleavage" activities of foot-and-mouth disease virus 2A site-directed mutants and naturally occurring "2A-like" sequences. *The Journal of General Virology*, *82*(5), 1027–1041. https://doi.org/10.1099/0022-1317-82-5-1027

Doudna, J. A., & Charpentier, E. (2014). Genome editing. The new frontier of genome engineering with CRISPR-Cas9. *Science*, *346*(6213), 1258096. https://doi.org/10.1126/science.1258096

Fong, J. H. C., & Ceroni, F. (2025). Transgene integration in mammalian cells: The tools, the challenges, and the future. *Cell Systems*, *16*(12), 101426. https://doi.org/10.1016/j.cels.2025.101426

Golosova, O., Henderson, R., Vaskin, Y., Gabrielian, A., Grekhov, G., Nagarajan, V., Oler, A. J., Quiñones, M., Hurt, D., Fursov, M., & Huyen, Y. (2014). Unipro UGENE NGS pipelines and components for variant calling, RNA-seq and ChIP-seq data analyses. *PeerJ*, *2*(1), e644. https://doi.org/10.7717/peerj.644

Gwon, L. W., Badon, I. W., Lee, Y., et al. (2025). Advances in large-scale DNA engineering with the CRISPR system. *Experimental & Molecular Medicine*, *57*, 1902–1912. https://doi.org/10.1038/s12276-025-01530-0

Guo, X.-Y., Gao, X.-D., & Fujita, M. (2021). Sulfation of a FLAG tag mediated by SLC35B2 and TPST2 affects antibody recognition. *PLoS ONE, 16*(5),0250805. https://doi.org/10.1371/journal.pone.0250805

Hackett, P. B., Largaespada, D. A., & Cooper, L. J. N. (2010). A transposon and transposase system for human application. *Molecular Therapy*, *18*(4), 674–683. https://doi.org/10.1038/mt.2010.2

Hsu, P. D., Lander, E. S., & Zhang, F. (2014). Development and applications of CRISPR-Cas9 for genome engineering. *Cell*, *157*(6), 1262–1278. https://doi.org/10.1016/j.cell.2014.05.010

Hughes, R. A., & Ellington, A. D. (2017). Synthetic DNA synthesis and assembly: Putting the synthetic in synthetic biology. *Cold Spring Harbor Perspectives in Biology*, *9*(1), a023812. https://doi.org/10.1101/cshperspect.a023812

Hunter, M. R., Grimsey, N. L., & Glass, M. (2016). Sulfation of the FLAG epitope is affected by co-expression of G protein-coupled receptors in a mammalian cell model. *Scientific Reports, 6*, 27316. https://doi.org/10.1038/srep27316

Indo, S., Orellana-Serradell, O., Torres, M. J., Castellón, E. A., & Contreras, H. R. (2024). Overexpression of REST represses the epithelial–mesenchymal transition process and decreases the aggressiveness of prostate cancer cells. *International Journal of Molecular Sciences*, *25*(6), 3332. https://doi.org/10.3390/ijms25063332

Ivics, Z., Li, M. A., Mátés, L., Boeke, J. D., Nagy, A., Bradley, A., & Izsvák, Z. (2009). Transposon-mediated genome manipulation in vertebrates. *Nature Methods*, *6*(6), 415–422. https://doi.org/10.1038/nmeth.1332

Kalva, S., Boeke, J. D., & Mita, P. (2018). Gibson deletion: A novel application of isothermal in vitro recombination. *Biological Procedures Online, 20*(1), 2. https://doi.org/10.1186/s12575-018-0068-7

Kaufman, W. L., Kocman, I., Agrawal, V., Rahn, H. P., Besser, D., & Gossen, M. (2008). Homogeneity and persistence of transgene expression by omitting antibiotic selection in cell line isolation. *Nucleic Acids Research*, *36*(17), e111. https://doi.org/10.1093/nar/gkn508

Kim, J. H., Lee, S.-R., Li, L.-H., Park, H.-J., Park, J.-H., Lee, K. Y., Kim, M.-K., Shin, B. A., & Choi, S.-Y. (2011). High cleavage efficiency of a 2A peptide derived from porcine teschovirus-1 in human cell lines, zebrafish and mice. *PLoS ONE*, *6*(4), e18556. https://doi.org/10.1371/journal.pone.0018556

Knappik, A., & Plückthun, A. (1994). An improved affinity tag based on the FLAG peptide for the detection and purification of recombinant antibody fragments. *BioTechniques*, *17*(4), 754–761.

Lacoste, A., Berenshteyn, F., & Brivanlou, A. H. (2009). An efficient and reversible transposable system for gene delivery and lineage-specific differentiation in human embryonic stem cells. *Cell Stem Cell*, *5*(3), 332–342. https://doi.org/10.1016/j.stem.2009.07.011

Lee, J. H., Chai, Y. G., & Hersh, L. B. (2000). Expression patterns of mouse repressor element-1 silencing transcription factor 4 (REST4) and its possible function in neuroblastoma. *Journal of Molecular Neuroscience*, *15*(3), 205–214. https://doi.org/10.1385/jmn:15:3:205

Lehner, P. J. (2025). Silencing by the HUSH epigenetic transcriptional repressor complex. *Annual Review of Biochemistry*, *94*(1), 361–386. https://doi.org/10.1146/annurev-biochem-020425-045352

Li, R., Zhuang, Y., Han, M., Xu, T., & Wu, X. (2013). PiggyBac as a high-capacity transgenesis and gene-therapy vector in human cells and mice. *DMM Disease Models and Mechanisms*, *6*(3), 828–833. https://doi.org/10.1242/dmm.010827

Lim, C. T., Lim, C. W., Huang, T., Ismail, E. N., Reisi, P., Cheah, P. S., & Ling, K. H. (2025). The regulatory roles of REST in the synaptic development, function and related neurological disorders. *Journal of Neurochemistry*, *169*(6), e70132. https://doi.org/10.1111/jnc.70132

Liu, X., Yan, J., Liu, F., Zhou, P., Lv, X., Cheng, N., & Liu, L. (2022). Overexpression of REST Causes neuronal injury and decreases cofilin phosphorylation in mice. *Journal of Alzheimer's Disease*, *87*(2), 873–886. https://doi.org/10.3233/jad-210285

Lu, T., Aron, L., Zullo, J., Pan, Y., Kim, H., Chen, Y., Yang, T. H., Kim, H. M., Drake, D., Liu, X. S., Bennett, D. A., Colaiácovo, M. P., & Yankner, B. A. (2014). REST and stress resistance in ageing and Alzheimer's disease. *Nature*, *507*(7493), 448–454. https://doi.org/10.1038/nature13163

Matasci, M., Bachmann, V., Baldi, L., Hacker, D. L., De Jesus, M., & Wurm, F. M. (2011). CHO cell lines generated by PiggyBac transposition. *BMC Proceedings*, *5*(8), 1–2. https://doi.org/10.1186/1753-6561-5-s8-p31

Mátés, L., Chuah, M. K. L., Belay, E., Jerchow, B., Manoj, N., Acosta-Sanchez, A., Grzela, D. P., Schmitt, A., Becker, K., Mát-rai, J., Ma, L., Samara-Kuko, E., Gysemans, C., Pryputniewicz, D., Miskey, C., Fletcher, B., VandenDriessche, T., Ivics, Z., & Izsvák, Z. (2009). Molecular evolution of a novel hyperactive Sleeping Beauty transposase enables robust stable gene transfer in vertebrates. *Nature Genetics*, *41*(6), 753–761. https://doi.org/10.1038/ng.343

McInerney, P., Adams, P., & Hadi, M. Z. (2014). Error rate comparison during polymerase chain reaction by DNA polymerase. *Molecular Biology International*, *2014*(1), 287430. https://doi.org/10.1155/2014/287430

Meyer, K., Feldman, H. M., Lu, T., Drake, D., Lim, E. T., Ling, K. H., Bishop, N. A., Pan, Y., Seo, J., Lin, Y. T., Su, S. C., Church, G. M., Tsai, L. H., & Yankner, B. A. (2019). REST and neural gene network dysregulation in iPSC models of Alzheimer's disease. *Cell Reports*, *26*(5), 1112-1127.e9. https://doi.org/10.1016/J.CELREP.2019.01.023

Nakazawa, Y., Saha, S., Galvan, D. L., Huye, L. E., Dotti, G., Foster, A. E., Vera, J. F., Manuri, P. R., June, C. H., Rooney, C. M., Wilson, M. H., & Savoldo, B. (2013). Evaluation of long-term transgene expression in piggyBac-modified human T lymphocytes. *Journal of Immunotherapy, 36*(1), 3–10. https://doi.org/10.1097/CJI.0b013e3182791234

Nechiporuk, T., McGann, J., Mullendorff, K., Hsieh, J., Wurst, W., Floss, T., & Mandel, G. (2016). The REST remodeling complex protects genomic integrity during embryonic neurogenesis. *eLife*, *5*, e09584. https://doi.org/10.7554/elife.09584

Okonechnikov, K., Golosova, O., Fursov, M., Varlamov, A., Vaskin, Y., Efremov, I., German Grehov, O. G., Kandrov, D., Rasputin, K., Syabro, M., & Tleukenov, T. (2012). Unipro UGENE: a unified bioinformatics toolkit. *Bioinformatics*, *28*(8), 1166–1167. https://doi.org/10.1093/bioinformatics/bts091

Parekh, U., Wu, Y., Zhao, D., Worlikar, A., Shah, N., Zhang, K., & Mali, P. (2018). Mapping cellular reprogramming via pooled overexpression screens with paired fitness and single-cell RNA-sequencing readout. *Cell Systems*, *7*(5), 548–555.e8. https://doi.org/10.1016/j.cels.2018.10.008

Perycz, M., Dabrowski, M. J., Jardanowska-Kotuniak, M., Roura, A. J., Gielniewski, B., Stepniak, K., Dramiński, M., Ciechomska, I. A., Kaminska, B., & Wojtas, B. (2024). Comprehensive analysis of the REST transcription factor regulatory networks in IDH mutant and IDH wild-type glioma cell lines and tumors. *Acta Neuropathologica Communications*, *12*(1), 1–29. https://doi.org/10.1186/s40478-024-01779-y

Randolph, L. N., Bao, X., Zhou, C., & Lian, X. (2017). An all-in-one, Tet-On 3G inducible PiggyBac system for human pluripotent stem cells and derivatives. *Scientific Reports*, *7*(1), 1–8. https://doi.org/10.1038/s41598-017-01684-6

Rose, R., Golosova, O., Sukhomlinov, D., Tiunov, A., & Prosperi, M. (2019). Flexible design of multiple metagenomics classification pipelines with UGENE. *Bioinformatics*, *35*(11), 1963–1965. https://doi.org/10.1093/bioinformatics/bty901

Sandoval-Villegas, N., Nurieva, W., Amberger, M., & Ivics, Z. (2021). Contemporary transposon tools: A review and guide through mechanisms and applications of *Sleeping Beauty*, *piggyBac* and *Tol2* for genome engineering. *International Journal of Molecular Sciences*, *22*(10), 5084. https://doi.org/10.3390/ijms22105084

Schmidt, P. M., Sparrow, L. G., Attwood, R. M., Xiao, X., Adams, T. E., & McKimm-Breschkin, J. L. (2012). Taking down the FLAG! How insect cell expression challenges an established tag-system. *PLoS ONE*, *7*(6), e37779. https://doi.org/10.1371/journal.pone.0037779

Tan, E., Chin, C. S., Lim, Z. F. S., Ng, S. K., & Hew, C. L. (2021). HEK293 cell line as a platform to produce recombinant proteins and viral vectors. *Frontiers in Bioengineering and Biotechnology*, *9*, 796991. https://doi.org/10.3389/fbioe.2021.796991

Thompson, J. R., Marcelino, L. A., & Polz, M. F. (2002). Heteroduplexes in mixed-template amplifications: Formation, consequence and elimination by "reconditioning PCR". *Nucleic Acids Research*, *30*(9), 2083–2088. https://doi.org/10.1093/nar/30.9.2083

Turchiano, G., Andrieux, G., Klermund, J., Blattner, G., Pennucci, V., El Gaz, M., Monaco, G., Poddar, S., Mussolino, C., Cornu, T. I., & Cathomen, T. (2014). Genomic analysis of Sleeping Beauty transposon integration in human somatic cells. *PLoS ONE*, *9*(11), e112712. https://doi.org/10.1371/journal.pone.0112712

Wilber, A., Linehan, J. L., Tian, X., Woll, P. S., Morris, J. K., Belur, L. R., McIvor, R. S., & Kaufman, D. S. (2007). Efficient and stable transgene expression in human embryonic stem cells using transposon-mediated gene transfer. *Stem Cells*, *25*(11), 2919–2927. https://doi.org/10.1634/stemcells.2007-0026

Wilson, M. H., Coates, C. J., & George, A. L., Jr. (2007). PiggyBac transposon-mediated gene transfer in human cells. *Molecular Therapy*, *15*(1), 139–145. https://doi.org/10.1038/sj.mt.6300028

Wu, S. C. Y., Meir, Y. J. J., Coates, C. J., Handler, A. M., Pelczar, P., Moisyadi, S., & Kaminski, J. M. (2006). PiggyBac is a flexible and highly active transposon as compared to Sleeping Beauty, Tol2, and Mos1 in mammalian cells. *Proceedings of the National Academy of Sciences of the United States of America*, *103*(41), 15008–15013. https://doi.org/10.1073/pnas.0606979103

Zhang, P., Casaday-Potts, R., Precht, P., Jiang, H., Liu, Y., Pazin, M. J., & Mattson, M. P. (2011). Nontelomeric splice variant of telomere repeat-binding factor 2 maintains neuronal traits by sequestering repressor element 1-silencing transcription factor. *Proceedings of the National Academy of Sciences of the United States of America*, *108*(39), 16434–16439. https://doi.org/10.1073/pnas.1106906108

Zhao, S., Jiang, E., Chen, S., Gu, Y., Shangguan, A. J., Lv, T., Luo, L., & Yu, Z. (2016). PiggyBac transposon vectors: the tools of the human gene encoding. *Translational Lung Cancer Research*, *5*(1), 120. https://doi.org/10.3978/J.ISSN.2218-6751.2016.01.05

Zhao, Y., Zhu, M., Yu, Y., Qiu, L., Zhang, Y., He, L., & Zhang, J. (2017). Brain REST/NRSF is not only a silent repressor but also an active protector. *Molecular Neurobiology*, *54*(1), 541–550. https://doi.org/10.1007/S12035-015-9658-4